SUPPORTING INFORMATION

Polymer-protein conjugates relaxation dynamics: polymer solvation enhances the overall protein flexibility

Daniela Russo[1,2*], MariePlazanet[3,4], Jose Teixeira[5], Martine Moulin[6,7] ,Michael Härtlein[6,7]Frederik R. Wurm[8], Tobias Steinbach[8]

[1] CNR-IOM(Italy), c/o Institut Laue-Langevin, Grenoble, France

[2]Institut Lumière Matière, Université de Lyon, Lyon, France

[3]Physics Department, Universita' degli Studi di Perugia, Italy

[4]LIPhy, CNRS and Université Grenoble Alpes, France

[5]Laboratoire Léon Brillouin, CEA and CNRS, Gif Sur Yvette, France

[6]ILL Deuteration Laboratory, Partnership for Structural Biology, Grenoble, France.

[7]Life Sciences Group, Institut Laue-Langevin, Grenoble, France

[8]Max Planck Institute for Polymer Research, Mainz, Germany

To whom correspondence should be addressed.russo@ill.fr

1. MBP deuteration, purification and Characterization

1.1 Maltose Binding Protein

Maltose-binding protein (MBP), a well-studied soluble protein, is essential for the energy-dependent translocation of maltose and maltodextrins through the cytoplasmic membrane. It binds maltose with a K_D of around 1μM and is constructed of two globular domains connected by a three-stranded hinge, with the ligand-binding site located in the cleft between the two domains. MBP has been crystallized in two conformations: a ligand bound "closed" form[1] and a ligand-free "open" form [2]; these differ primarily by a rigid-body rotation of one domain relative to the other, which results in opening or closing of the ligand-binding cleft. Both samples in our

study, i.e.perdeuterated and unlabeled MBP, contained the ligand-free form.

1.2 Expression and purification of perdeuterated and unlabeled MBP

Perdeuterated and unlabeled MBP was expressed in the Deuteration Laboratory of the Institute Laue-Langevin (ILL), Grenoble, France, essentially as described by Wood et al.[3]. Briefly, the coding sequence for the mature form of *E.coli* MBP was subcloned from pMAL-c2E vector (New England Biolabs into pET-28a (Novagen) vector that confers kanamycin resistance to the expression construct and an N-terminal histidine-tag to MBP to facilitate large-scale purification. Perdeuterated histidine-tagged MBP was obtained by expression in *Escherichia coli* BL21(DE3) using high cell density cultures. Cells were grown in minimal medium under kanamycin selection and d_8-glycerol (Euriso-Top, France) as carbon source [4]. Adaptation of BL21(DE3) cells to deuterated minimal medium was achieved by a multi-stage adaptation process (1.5 L of deuterated medium was inoculated with 100 mL preculture of adapted cells in a 3 L fermenter (Labfors, Infors). During the batch and fed-batch phases the pH was adjusted to 6.9 (by addition of NaOD) and the temperature was adjusted to 303 K. Stirring was adjusted to ensure a dissolved oxygen tension (DOT) of 30%. The fed-batch phase was initiated when the optical density at 600 nm reached a value of about 3, d_8-glycerol was added to the culture to keep the growth rate stable during fermentation. When OD 600 reached about 14, MBP overexpression was induced by the addition of 0.5 mM IPTG and incubation continued for 24 h. Cells (about 50g of wet weight expressing roughly 500mg of d-MBP) were then harvested, washed with 10 mM HEPES (pH 6.4), and stored at 193 K. D-MBP was purified in one step using immobilized metal ion affinity chromatography (IMAC) on TALON (Clontech). All buffers used during purification

were made with H_2O. Protein purity was assessed by SDS-PAGE and the molecular weight of perdeuterated*E.coli* MBP was determined by MALDI mass spectrometry. Hydrogenated MBP (H-MBP) was expressed at 303 K using LB medium in flask cultures and induced with 1mM IPTG when the OD_{600} reached the value of 0.8. H-MBP was purified in a similar way as the perdeuterated MBP. About 300mg were obtained from 2L of culture. Both MBP isotopic forms were dialysed against 100mM borate buffer pH 8.5

2. Synthesis and characterization of $PMeEP^H$/ $PMeEP^D$

2.1 Materials.

Solvents were purchased from Sigma Aldrich (Germany) and used as received, unless otherwise stated.2-Methyl-1,3,2-dioxaphospholane 2-oxide (MeEP) was prepared as reported previously[5].1,8-Diazabicyclo[5.4.0]undec-7-ene (DBU) was purchased from Sigma-Aldrich (Germany), distilled from CaH_2 prior to use and stored over molecular sieve (4 Å).2-(Benzyloxy)ethanol was purchased from ABCR and distilled from sodium prior to use.Acetonitrile (ACN), dichloromethane (DCM), dioxane and toluene were stored over molecular sieve, Dulbecco's phosphate buffered saline (D-PBS),ammonium acetate and sodium tetraboratedecahydrate were used as received from Sigma-Aldrich (Germany).Ammonium bicarbonate was used as received from Fisher Scientific. *N*,*N*′-disuccinimidyl carbonate (DSC)was used as received from Acros Organics (Germany). BSA, *N*-Hdroxysuccinimide

(NHS), Deuterated solvents were purchased from Deutero GmbH (Kastellaun, Germany) and used as received.Ultrapure water with a resistivity of 18.2 $M\Omega cm^{-1}$ (Milli-Q, Millipore®) was used to prepare buffers.

2.2 Instrumentation.

The ^{1}H-, ^{13}C- and ^{31}P-NMR experiments were acquired on a 400 MHz Bruker AMX system. The temperature was kept at 298.3 K and calibrated with a standard ^{1}H methanol NMR sample using the topspin 3.0 software (Bruker). ^{13}C-NMR spectra were referenced internally to solvent signals. ^{31}P-NMR spectra were referenced externally to phosphoric acid. The ^{13}C NMR (101 MHz) and ^{31}P NMR (168 MHz) measurements were obtained with a ^{1}H powergate decoupling method using 30° degree flip angle.

Size exclusion chromatography (SEC) was performed withphosphate buffered saline (PBS, 100 mM phosphate, 50 mM sodium chloride, pH 6.5)as eluent.BSA samples were separated over a set of HEMA-Bio columns (40/100/1000) with 10 μm particles with a length of 300 mm and an internal diameter of 8 mm (MZ-Analysentechnik) providing an effective molecular weight range of 2000−3.000.000 at a flow rate of 1.0 ml min^{-1} (Agilent 1260 HPLC). UC samples were separated over a Superdex 200 10/300 GL column with 13 μm particles with a length of 300 mm and an internal diameter of 10 mm (GE Healthcare) providing an effective molecular weight range of 10,000−600,000 at a flow rate of 0.75 ml min^{-1} (Agilent 1260 HPLC). Each sample injection was 50 μL at a protein concentration of 2 mg mL^{-1}. Elution profiles for mass analysis were detected using an ultraviolet–visible detector (280 nm, Agilent 1260), a Wyatt miniDAWN TREOS MALLS detector, a Wyatt ViscoStar II on-line differential viscometer and a differential refractometer (Agilent 1260). Using the elution-profile data the weight-averaged molecular mass

(M_w) was calculated with Astra 6.1.1 software (Wyatt Technologies) using a dn/dc of 0.1035 for PMeEP.

2.3 Synthesis of MeEP.

Hydrogenated monomer MeEP was prepared as describedbefore[5]. Partially deuterated MeEP-d_4 was preparedanalogously:briefly, a three-necked round bottom flask, equipped two dropping funnels, was charged with 50 mL dry THF and cooled to -21°C. Methylphosphonic dichloride (32.8 g, 247mmol) was dissolved in dry THF (230 mL) and transferred into one dropping funnel *via* a flame-dried stainless steel capillary. A solution of dry ethylene glycol-d_6(16.8g, 247mmol, purchased from Deutero GmbH, Kastellaun, Germany) and dry pyridine (39.0 g, 494mmol) in THF (170 mL) was transferred into the second dropping funnel *via* a flame-dried stainless steel capillary. Dropping speed was adjusted to be approximately equal for both mixtures. After complete addition the solution was stirred for 6 hours and stored over night at -28°C to facilitate the precipitation of the pyridiniumdeuterochloride. The precipitate was removed by filtration *via* a flame-dried Schlenk funnel and the solvent was removed *in vacuo*. Repeated fractionated distillation yielded the desired product (15.9 g, yield: 51%, b.p. 115°C / $1 \cdot 10^{-3}$ mbar). ^{1}H NMR (DMSO-d_6, ppm): δ 1.60 (d, J = 17.5 Hz, 3H, P-C$\underline{H}_3$).^{13}C NMR (DMSO-d_6, ppm): δ 66.05 (qi, J = 24 Hz,$\underline{C}D_2$-$\underline{C}D_2$), 11.38 (d, $^1J_{PC}$ = 131 Hz, P-$\underline{C}H_3$). ^{31}P{H} NMR (DMSO-d_6, ppm): δ48.5.

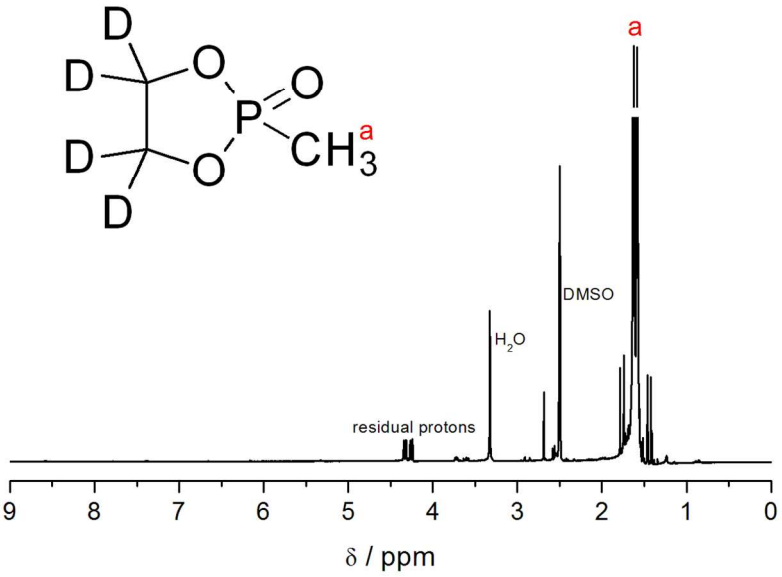

Figure S1. *^{1}H NMR spectrum (400 MHz, 298K) of deuterated MeEP (MeEP^{D})in DMSO-d_6.*

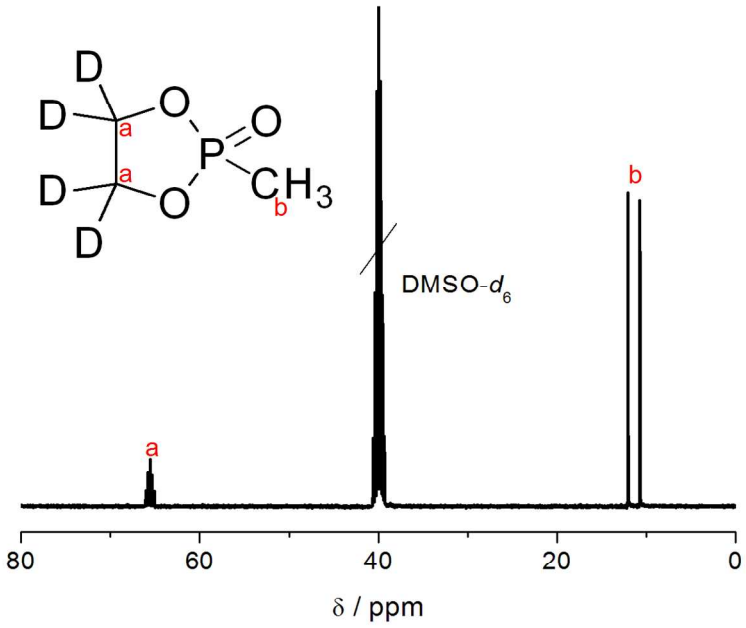

Figure S2. *^{13}C NMR (101 MHz, 298 K) spectrum of deuterated MeEPin DMSO-d_6.*

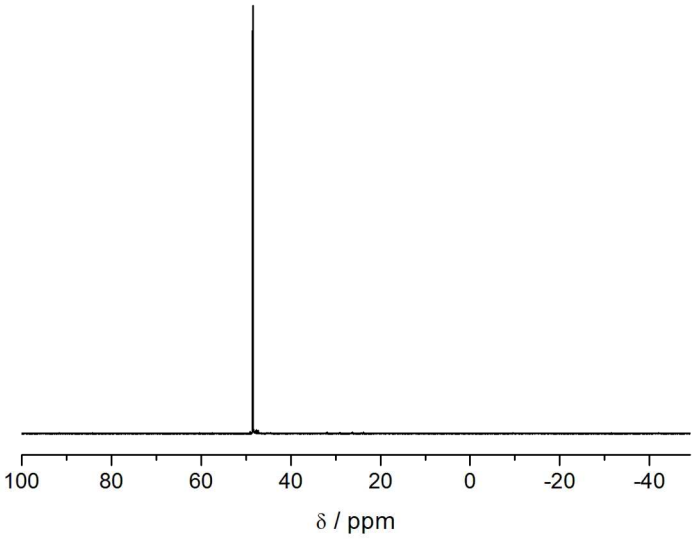

Figure S3. *$^{31}P\{H\}$ NMR (168 MHz, 298K) spectrum of deuterated MeEP in DMSO-d_6.*

2.4 Representative synthesis of PMeEP-SC.

The monomer MeEP(1.307 g, 10.7 mmol) was placed into a flame-dried Schlenk-tube, dissolved in 1 mL benzene and dried by repeated (three times) lyophilization. A stock solution of 2-(benzyloxy)ethanol in dichloromethane (0.2 M) was prepared and 1045 µL (209 µmol) were transferred to the monomer solution. The mixture was cooled to 0°C and the polymerization was started by the rapid addition (1570 µL, 314 µmol) of a dichloromethane stock solution of DBU (0.2 M). The polymerization was terminated after 80 minutes (~ 80% conversion as shown before) by the rapid addition of a 10-fold excess of *N*,*N*′-disuccinimidyl carbonate (DSC)dissolved in cold, dry acetonitrile (535 mg in 8 mL ACN). After 30 minutesthe polymer was purified by precipitation in cold diethyl ether and stored until usage

at -28°C. PMeEP$_{54}$-SC ^{1}H NMR (DMSO-d_6, ppm): δ7.43 – 7.20 (m, 5H, Ar), 4.52 (s, 2H, Bn-O-C$\underline{H}_2$), 4.39 – 4.00 (m, 216H, O-C$\underline{H}_2$-C$\underline{H}_2$-O), 2.81 (s, 4H, SC-group), 1.51 (d, J = 18 Hz, 170H, P-C$\underline{H}_3$). ^{13}C NMR (DMSO-d_6, ppm):δ169.94 (s, O$\underline{C}$-CH$_2$-CH$_2$-$\underline{C}$O), 151.30 (s, O-($\underline{C}$O)-O), 138.21 (Ar), 128.31 (Ar), 127.61 (Ar), 127.53 (Ar), 71.99 (Ar-$\underline{C}$H$_2$-O), 68.91 (d, J = 6.2 Hz, Ar-CH$_2$-O-$\underline{C}$H$_2$), 66.76 (d, J = 6.4 Hz, Ar-CH$_2$-O-CH$_2$-$\underline{C}$H$_2$), 64.24 (br. s, backbone), 60.36 (d, J = 6.5 Hz, $\underline{C}$H$_2$-O-CO), 25.41 (s, OC-$\underline{C}$H$_2$-$\underline{C}$H$_2$-CO), 10.39 (d, J = 140.8 Hz, P-CH$_3$).^{31}P NMR (DMSO-d_6, ppm): δ 32.0 (backbone), 31.6 (terminal P-CH$_3$).

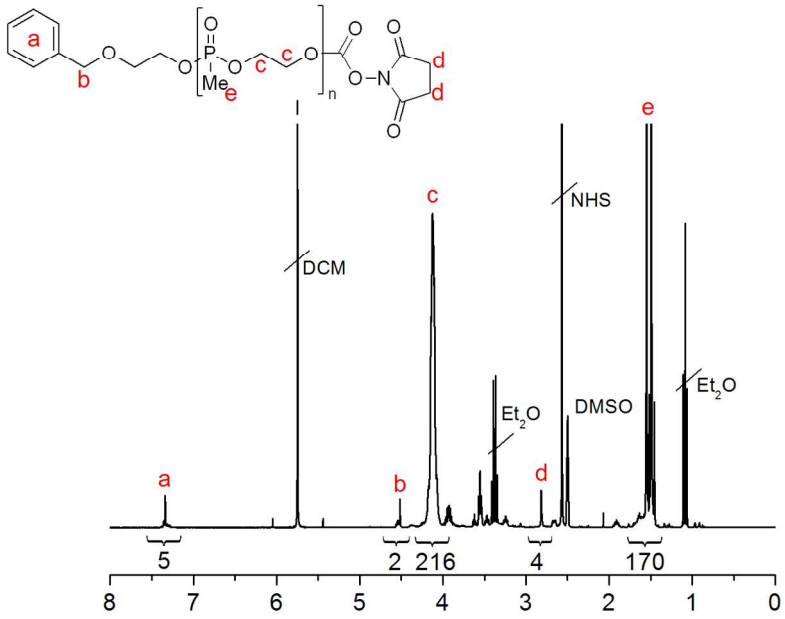

Figure S4. *Representative ^{1}H NMR spectrum of PMeEP-SCin DMSO-d_6.*

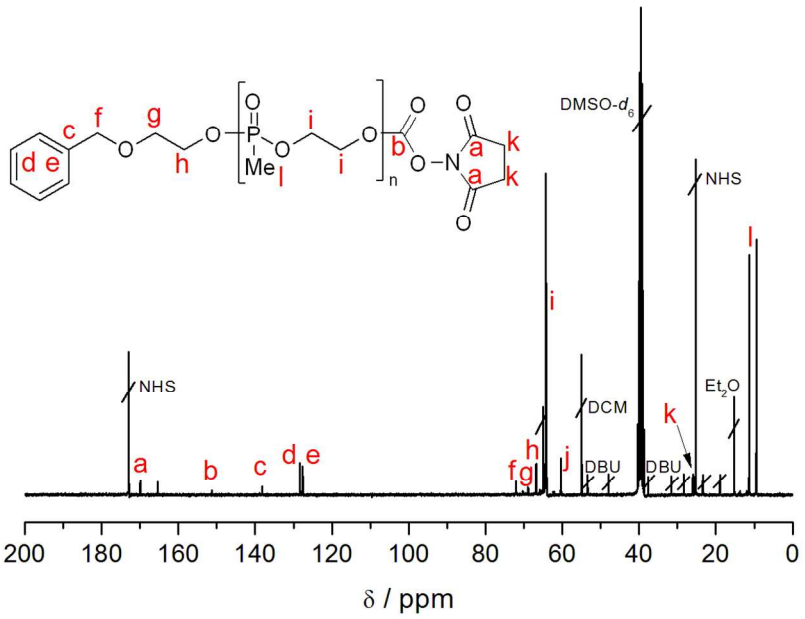

Figure S5. *Representative ^{13}C NMR spectrum of PMeEP-SCin DMSO-d_6.*

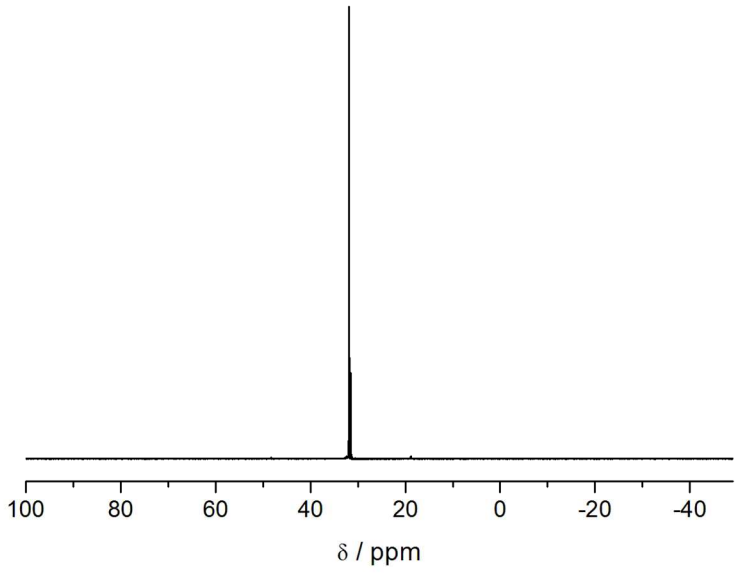

Figure S6. *Representative ^{31}P NMR spectrum of PMeEP-SCin DMSO-d_6.*

Table S1.

Amine-reactive hydrogenated and deuterated polymers synthesized in this study. Absolute molecular weights were determined via ^{1}H NMR spectroscopy by comparison of the integral of the aromatic protons at 7.43 – 7.20 ppm with the integral of the protons of the methylphosphonategroups of the repeating units at 1.51 ppm.

Polymer-Code	M_n^{NMR}
$PMeEP_{5k}^{H}$-SC	6.6 kDa
$PMeEP_{10k}^{H}$-SC	12.3 kDa
$PMeEP_{5k}^{D}$-SC	4.9 kDa
$PMeEP_{10k}^{D}$-SC	8.5 kDa

3. Polymer grafting on Maltose Binding Protein

3.1 Representative synthesis of MBP-PMeEP conjugate.

MBP-H (100 mg, 2.35µmol, 89.4 µmol NH_2-groups) was dissolved in 10 mL of borate buffer (100 mM, pH 8.5) and added to PMeEP-SC (1.118 g, 89.4 µmol). The mixture was allowed to react at 20°C for 2 hour shaking before repeated dialysis (3x 1 L H_2O, 25 000 MWCO) to remove excess polymer and NHS. Lyophilization yielded the colorless but still hydrated conjugate.

3.2 Characterization of the conjugates.

The molecular weight of the conjugates was determined by aqueous SEC. Samples were separated over a set of HEMA-Bio columns (40/100/1000, 10 µm particles) with a length of

300 mm and an internal diameter of 8 mm (MZ-Analysentechnik) providing an effective molecular weight range of 2000−3.000.000 at a flow rate of 1.0 ml min^{-1} (Agilent 1260 HPLC) in 100 mM phosphate, 50 mM sodium chloride buffer, pH 6.5.Each sample injection was 20 µL at a protein concentration of 2 mg mL^{-1}. Elution profiles for mass analysis were detected using an ultraviolet–visible detector (280 nm, Agilent 1260), a Wyatt miniDAWN TREOS MALLS detector and a differential refractometer (Agilent 1260). Using the elution-profile data the number-averaged molecular mass (M_n) was calculated with Astra 6.1.1 software (Wyatt Technologies).

Table S2.

MBP-conjugates synthesized in this study. Molecular weights were calculated by on-line light scattering in aqueous buffer solution.

Code	M_n	# polymer chains attached
$PMeEP_{5k}^{H}$-MBP^{H}	54 kDa	2
$PMeEP_{10k}^{H}$-MBP^{H}	57 kDa	1-2
$PMeEP_{10k}^{D}$-MBP^{H}	59 kDa	2
$PMeEP_{10k}^{H}$-MBP^{D}	60 kDa	1-2

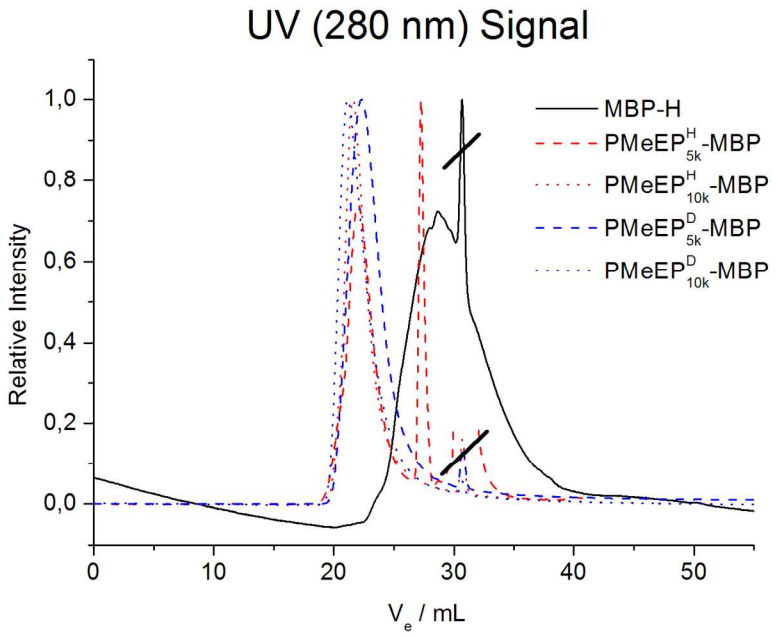

Figure S7. *UV-SEC traces of the unmodified MBP-H and the corresponding conjugates.*

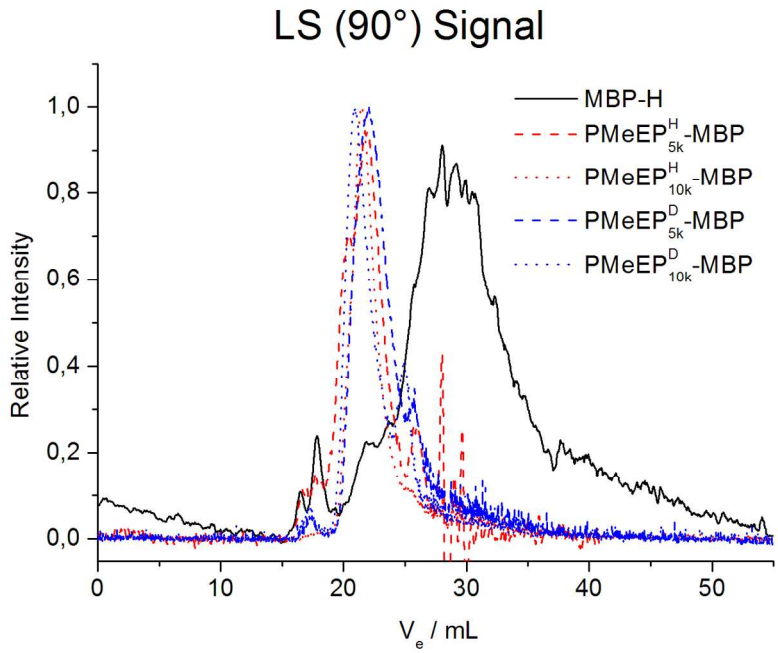

Figure S8. *LS-SEC traces of the unmodified MBP-H and the corresponding conjugates.*

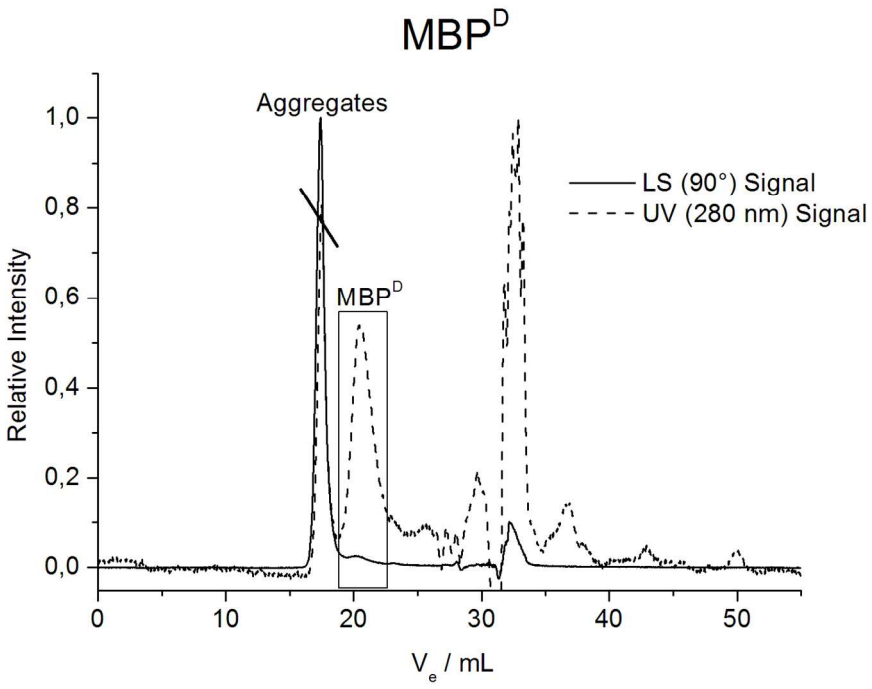

Figure S9. *SEC traces of MBP^D recorded with LS and UV detector.*

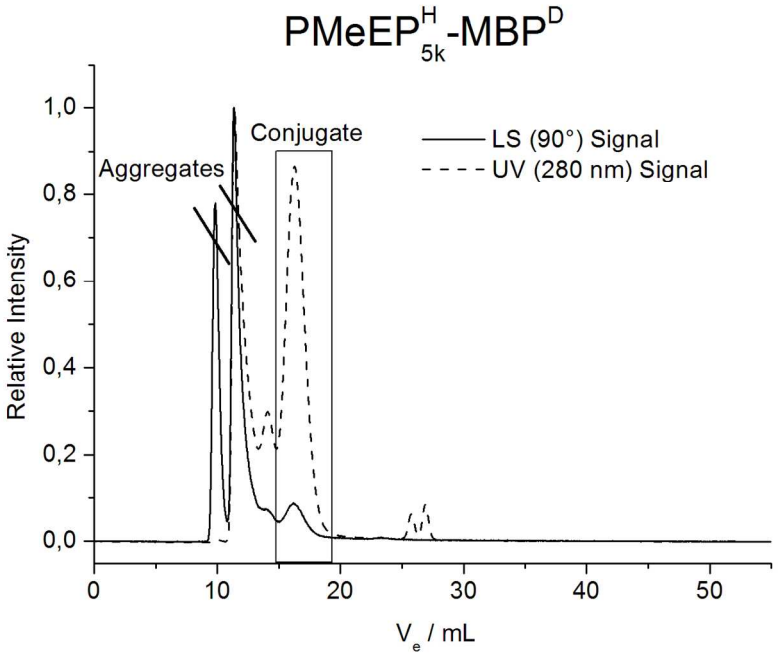

Figure S10. *SEC traces of $PMeEP_{5k}^H$-MBP^D recorded with LS and UC detector.*

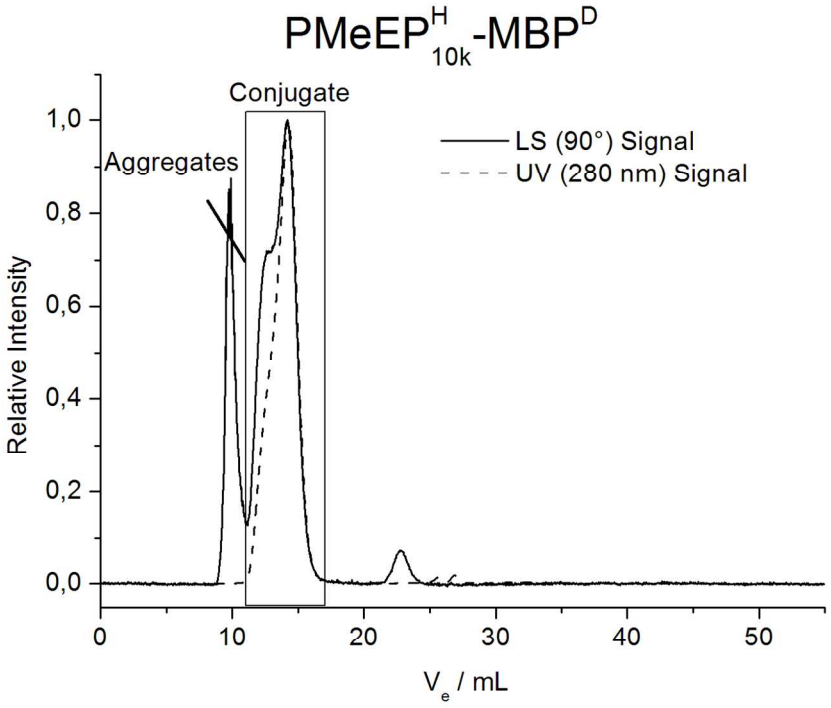

Figure S11. *SEC traces of PMeEP$_{10k}^{H}$-MBP^{D} recorded with LS and UC detector.*

4. Elastic and quasi-elastic neutron scattering experiment

Neutron scattering experiments were performed on the new high flux backscattering spectrometer IN16B[6] at ILL with energy resolution of 0.9 microeV. Elastic scans were recorded in a range of temperature between 50 and 300 K and a heating rate of 1.5 K/min, while quasi-elastic measurements were recorded only at room temperature for selected samples. The collected signal was measured over a wave vector Q range extending from 0.1 to 1.8 Å^{-1} where $Q = 4\pi\sin\theta/\lambda$ is the elastic momentum exchange, 2θ is the scattering angle and λ is the wavelength of the incident neutrons. All elastic and quasi-elastic spectra were corrected for detector efficiency and normalized using the respective measurement at 50 K, where the system is completely frozen. Samples were loaded into slab containers 0.1 mm tick. The resulting data were corrected and analyzed using the NCNR DAVE programs [7] and ILL LAMP programs [8]

4.1 Neutron scattering cross sections.

4.2

In the table S3 are summarized neutrons scattering cross sections useful for the data interpretation. Coherent and incoherent cross sections were calculated for (protonated or deuterated): MBP (from amino acid sequence), polymer for the two molecular weights ($C_8H_9O_2[C_3H_7O_3P]_nCHON$, with n=40 and 80 for 5 and 10 kDa respectively), and water molecule. For each samples, we calculated the fraction of the signal arising from each component: the polymer, protein and water molecules. Finally, the ratio between the total coherent and the total incoherent cross section, for each sample, has been also calculated. The fraction of coherent (or incoherent) signal arising from one component is calculated as the ratio between the cross section X of this component over the cross section of the whole sample:

$$r_s = X_{i,\,s}/(X_{prot,\,s} + N*X_{pol,\,s} + h*X_{water,\,s})$$

s=coherent (or incoherent) cross section, i=protein, N*polymer or h*water; N is the number of attached polymer, and *h* the number of hydration water: $h=0.4*M_{conjugate}/M_{water}$.

The ratio between coherent and incoherent for a given sample is calculated using the following equation:

$$(X_{prot}+N*X_{pol}+h*X_{water})_{coh}/(X_{prot}+N*X_{pol}+h*X_{water})_{incoh}.$$

Because the maximum of the structure factor of water, at low temperature, is around 1.7 A^{-1}, at the limit of the investigated Q-range, its coherent scattering can be neglected in the analysis. The signal of samples containing MBP(H) are therefore dominated by incoherent scattering, which is Q independent. The incoherent cross sections can therefore be simply added in the right

proportions to take into account the contribution of each component in the measured signal. For samples containing MBP(D), the coherent scattering of the protein cannot be neglected anymore, The scattered intensity is completely due to the form factor of the protein because the interactions are negligible at these concentrations.. Combining the various numbers, we obtain that in the dry MBP(D)-PMeEP(H)$_{10kDa}$ sample, the signal is roughly equally distributed between the (coherent) signal from the protein and the (incoherent) signal from the polymer. In the corresponding hydrated sample, it is roughly composed by 45% of (incoherent) signal from the polymer and 30% from the protein.

TABLE S3

Coherent and incoherent neutron scattering cross sections for all samples. In bold are the signal contributions of polymer and protein that may be considered for each sample.

sample description	**σ_coherent**	**σ _incoherent**	
PMeEP(H) 5kDa	1884.63	23175.68	
PMeEP(H) 10kDa	3683.55	45551.74	
PMeEP(D) 10kDa	4912.35	20633.34	
MBP(H)	26804.67	298557.71	
MBP(D)	41139.39	7869.00	
H2O	7.75	159.83	**ratio (total) coherent/incoherent**
Dry samples			
MBP(H)-PMeEP(H) 10kDa			0.09
Fraction signal from protein	0.78	**0.77**	
Fraction signal from polymer	0.22	**0.23**	
MBP(H)-PMeEP(H) 5kDa			0.09
Fraction signal from protein	0.88	**0.87**	
Fraction signal from polymer	0.12	**0.13**	
MBP(H)-PMeEP(D)10kDa			0.11

Fraction signal from protein	0.73	**0.88**	
Fraction signal from polymer	0.27	**0.12**	
MBP(D)-PMeEP(H)10kDa			**0.49**
Fraction signal from protein	**0.85**	0.08	
Fraction signal from polymer	0.15	**0.92**	
Hydrated samples			
MBP(H)-PMeEP(H) 10kDa			0.15
Fraction signal from protein	0.46	**0.75**	
Fraction signal from polymer	0.13	**0.23**	
Fraction signal from water	0.41	0.02	
MBP(H)-PMeEP(H) 5kDa			0.15
Fraction signal from protein	0.53	**0.85**	
Fraction signal from polymer	0.07	**0.13**	
Fraction signal from water	0.40	0.02	
MBP(H)-PMeEP(D) 10kDa			0.17
Fraction signal from protein	0.44	**0.86**	
Fraction signal from polymer	0.16	**0.12**	
Fraction signal from water	0.39	0.02	
MBP(D)-PMeEP(H) 10kDa			
Fraction signal from protein	**0.57**	0.07	0.69
Fraction signal from polymer	0.10	**0.87**	(without water : **0.49**)
Fraction signal from water	0.33	0.06	

4.2Elastic incoherent neutron scattering experiments and data analysis

Elastic and quasielastic neutron scattering experiments have been used to investigate the polymer-protein dynamics, flexibility and dynamical transition of completely hydrogenated and

partially deuterated complexes. Neutrons interact strongly with hydrogen nuclei, which are the main atoms present in protein structure and participate in bond formation, water and chain dynamics. In particular, incoherent scattering, a specificity of the interaction of neutrons with matter, gives detailed information about individual motions taking place at the molecular level. Deuteration labeling allows to disentangle motions and to study separately the different dynamics components in a complex system.

Elastic scans were carried out using the so-called fixed window scans, in which only the elastic intensity, convoluted with the instrumental function, is measured as a function of the temperature. When the diffusive motions of the H atoms are very slow, the broadening of the resolution is not observable, and the intensity is assimilated to the purely elastic one.. However, the measured intensity changes with temperature, (immobile atoms gives the maximum intensity while mobile atoms, on a timescale faster than the resolution, do not contribute anymore) what can be interpreted with the help of appropriate models. Despite its apparent simplicity, the results of elastic scans are very pertinent, and can be interpreted at least qualitatively, in many cases. Typically, a significant decrease of the intensity marks the onset of a relaxation process on the time scale of the instrument. For example, a sharp decrease of the peak intensity can be due to the onset of fast dynamics generating line widths eventually above the experimental resolution. Integrated elastic intensity (IEI) over the Q range enhances the features of some dynamical properties and do not require data manipulation as fitting procedure. The evaluation of the Q dependence of the scattering intensity gives access to the mean square displacement of the hydrogen atoms as a function of temperature. If we write

$$I(Q)/I(0)=\exp(-\langle u^2\rangle Q^{\wedge 2}/3) \quad (S1)$$

$\langle u^2 \rangle$ might be interpreted as the average radius of the region dynamically occupied by the hydrogen atoms. At low temperature $\langle u^2 \rangle Q^2$ corresponds to the Deby Waller factor, while rotational and translational motions will contribute when increasing the temperature. If the timescales of vibrational, rotational and translational motions are separated, the mean square displacements can be written as a sum of the three contributions:

$$\langle u^2 \rangle = \langle u_{DW}^2 \rangle + \langle u_{rot}^2 \rangle + \langle u_T^2 \rangle \quad \text{(S2)}$$

The quasi-elastic incoherent neutron scattering experiment measures the double differential incoherent scattering cross section:

$$\frac{d^2\sigma_{inc}}{dEd\Omega} = \frac{\sigma_{inc}}{4\pi}\frac{k_s}{k_i} NS_{inc}(Q,\omega) \quad \text{(S3)}$$

where σ_{inc} is the total incoherent scattering cross section per scatterer, N is the number of scatterers, k_i and k_s are the wave vectors of the incident and scattered neutrons, Q is the momentum transfer, ω is the energy transfer, and $S_{inc}(Q,\omega)$ is the incoherent dynamic structure factor. $S_{inc}(Q,\omega)$ probes both translational diffusion and rotational motions on the picosecond timescale[9].

The technique gives an averaged measurement of all relaxations occurring in the system. Our strategy therefore consists in qualitatively comparing the dynamics of the various samples through a global relaxation time.We analyzed the intermediate scattering function, I(Q,t), generated by the Fourier transform of $S(Q,\omega)$, using the DAVE fast Fourier transform utility[7].

The best fit to the long-time decay of $F_H(Q,t)$ was achieved using a single exponential.:

$$F_H(Q,t) = \exp\left[-(t/\tau)\right] \qquad \text{(S4)}$$

where τ is the characteristic relaxation time. Fitting results from a stretch exponential suggested β stretch factor close to one and equivalent relaxation time as inferred from eq (4). Double exponential has been also tested, however results were not satisfying.

4.3Elastic Intensity and Mean Square Displacement.

Examples of logarithms of the elastic intensities, vs Q^2, as a function of Temperature for dry and hydrated MBP protein and MBP(H)-PMeEP (H) $_{10KDa}$are represented in figure S12 a –d.

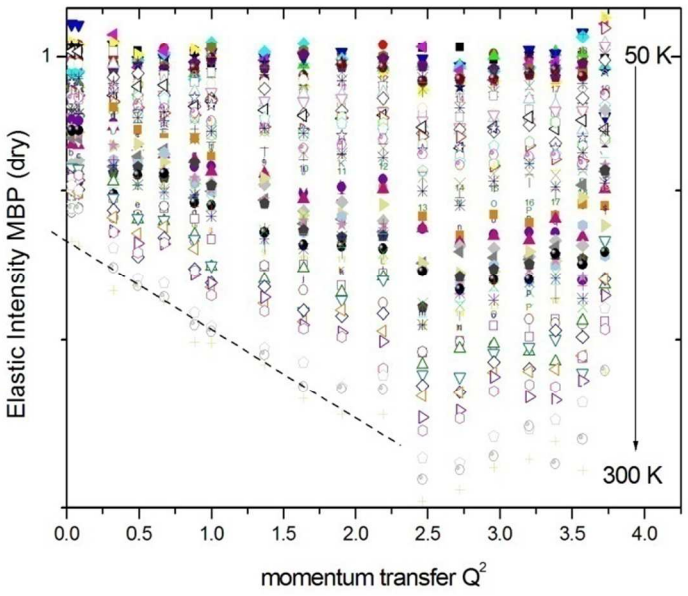

a)

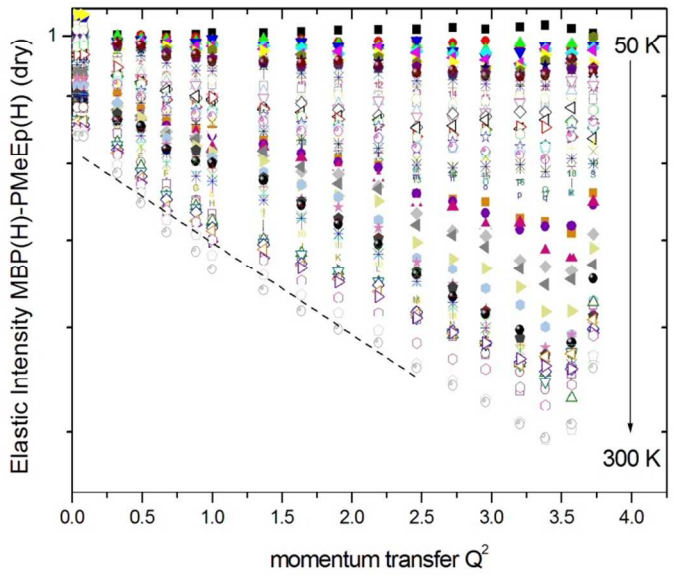
Elastic Intensity MBP(H)-PMeEp(H) (dry)
1
50 K
300 K
0.0
0.5
1.0
1.5
2.0
2.5
3.0
3.5
4.0
momentum transfer Q²

b)

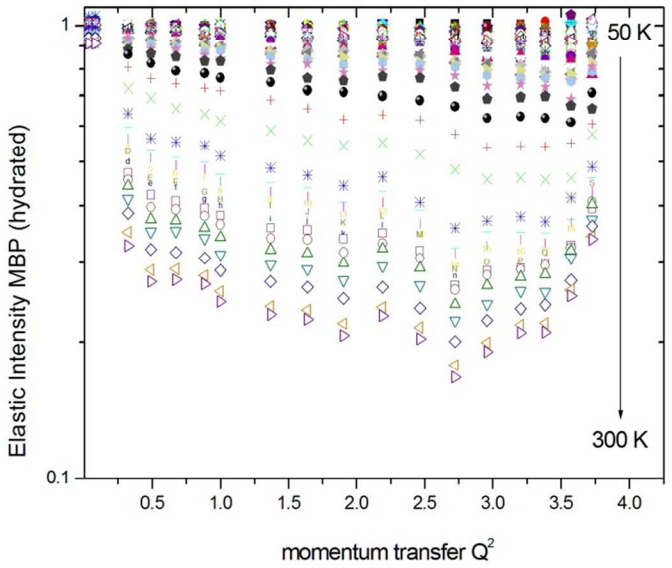
Elastic Intensity MBP (hydrated)
1
0.1
50 K
300 K
0.5
1.0
1.5
2.0
2.5
3.0
3.5
4.0
momentum transfer Q²

c)

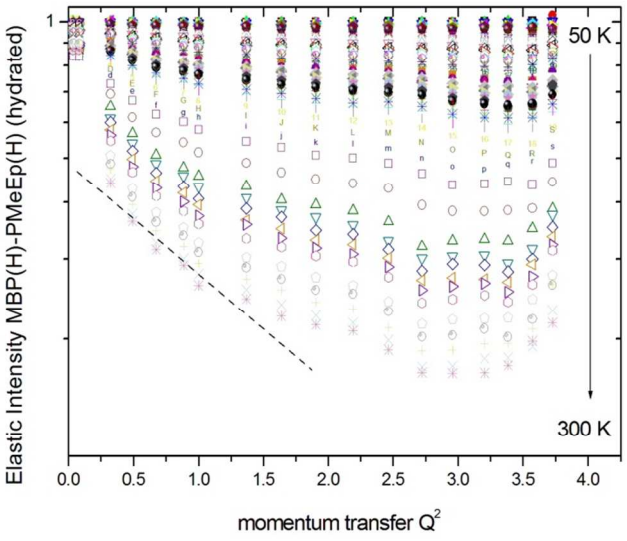

d)

Figure S12. *Elastic intensity against Q^2 of all dry (a,b) and hydrated (c,d) MB(a,c) and MBP(H)-PMeEP(H)$_{10KDa}$ (b,d), for all Temperature in the range between 50-300 K. The dashed lines correspond to linear fit to extract the MSD at given Temperature.*

The mean square displacement has been calculated using the ILL- LAMP package, using the expression in eq (1), where MSD =$<u^2>/3$. The fit has been performed fitting the data in thesmaller $Q^{\wedge 2}$ linear range(between $0.08< Q^2<1.0$-2.5 depending on the hydration level).Figure S2ashows the mean square displacement for the dry MBP protein,MBP(H)-PMeEP(H)$_{5kDa}$and PMeEP(H)$_{5kDa}$. The results are consistent with the integrated elastic intensity, showing that dry MBP is intrinsic of a lower MSD compare toMBP(H)-PMeEP(H)$_{5kDa}$conjugate and that in both case the dynamical transition is missing. The dry polymer presents a glass transition at around 240K

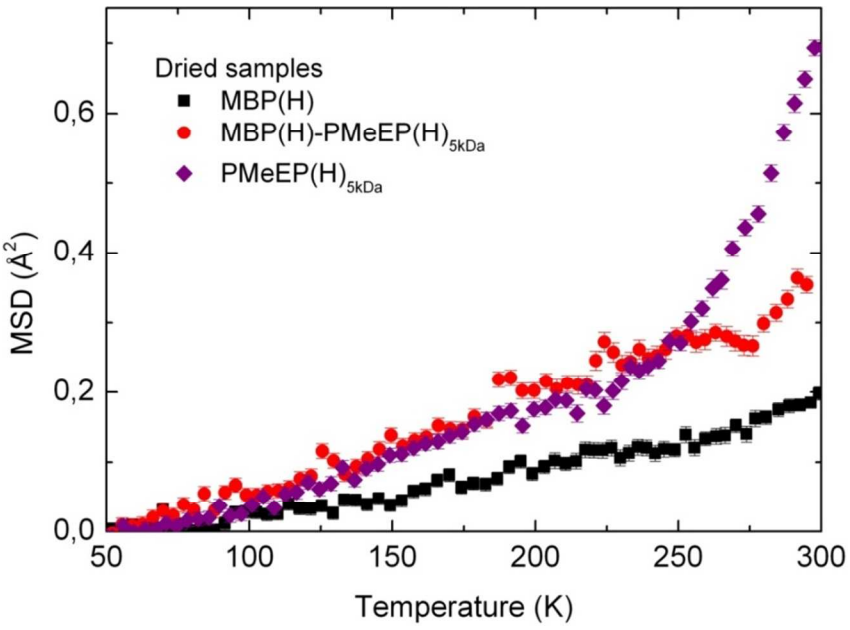

a)

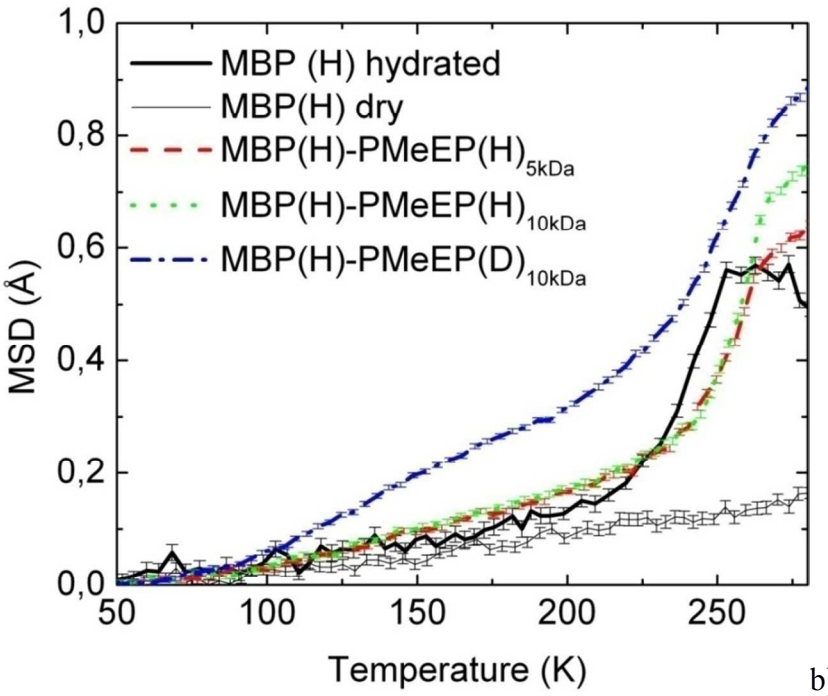

b)

Figure S13. *MSD of all dry (a) and hydrated conjugates (b) compare to dry MBP. In both dry and hydrated MSD, the vibrational, rotational and translational contributions are included. In Figure S13a) the polymer Glass transition is visible at 240 K, in Figure S13b) the dynamical transition of the conjugate is observed at T > 200 K.*

In the figure S13b are computed the MSD of hydrated samples. The protein MBP has already been characterized by elastic neutron scattering, in good agreement with the present data[3,10]. For a hydration of h=0.4, the native protein exhibits indeed a dynamical transition in the range of 200K. In Figure 4 of the manuscript we observe in the elastic intensity at ~260K, an abrupt break in smooth decrease.This translate in the Figure S13b) in a plateau in the MSD. This effect was already observed and reported in other hydrated proteins and systems[11,12]and cannot be assigned to the formation of ice due to an excess of water because Bragg peaks were not observed. It only appears in the D_2O hydrated protein above a given threshold of hydration (around 0.4), but its origin was not clarified yet. Instrument resolution limits could be also a possible explanation.

The MSD associated to the completely hydrogenated conjugates, at high and low molecular weight, differ only at higher temperature. TheMBP(H)-PMeEP$(D)_{10kDa}$in agreement to the IEI show a higher flexibility and a less pronounced transition compared to the native MBP.

4.4 Comparison Dry vs Hydrated of all Integrated Elastic Intensity

Figure S14 shows the comparison of all investigated sample with the respective dry and hydrated. All the samples have a regular dry/hydrated behavior except the MBP(D)-PMeEP$(H)_{10kDa}$ which seems to confirm that the dry sample eventually need to be re-measured or re-synthesized.If we define the temperature of the dynamical transition the temperature where the elastic intensity of the hydrated protein leaves the dry elastic curve we obtain the following Td: MBP =200 K; PMeEP$(H)_{5kDa}$ = 240K; MBP(H)-PMeEP$(H)_{10kDa}$=225 K; MBP(H)-PMeEP$(D)_{10kDa}$= 225 K; MBP(D)-PMeEP$(H)_{10kDa}$ = 225 K

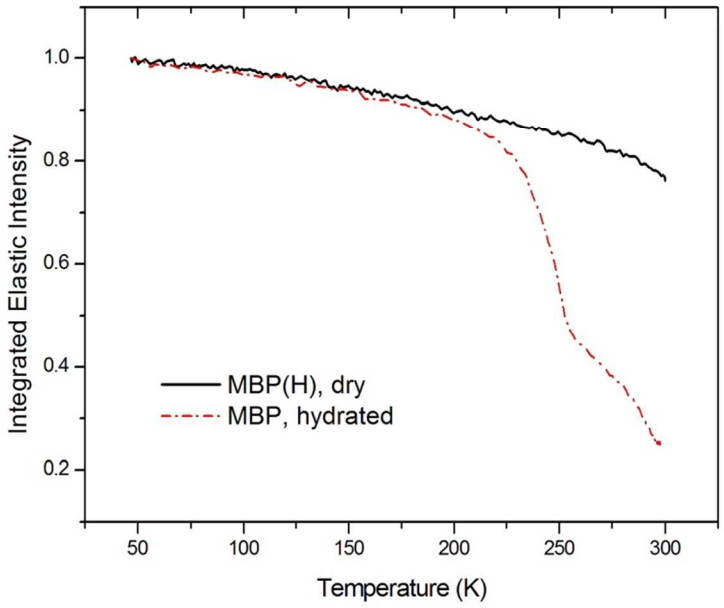
Integrated Elastic Intensity
1.0
0.8
0.6
0.4
0.2
50
100
150
200
250
300
Temperature (K)
MBP(H), dry
MBP, hydrated

a)

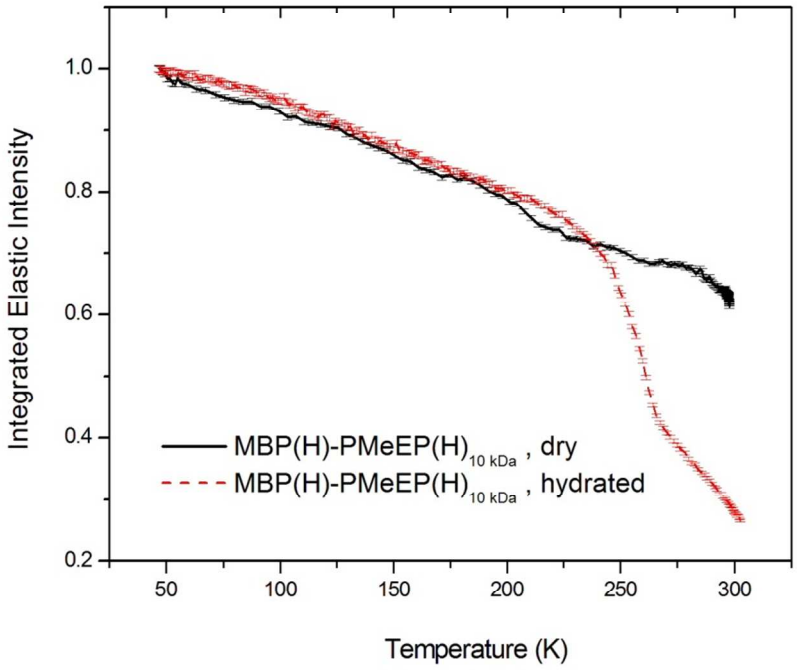
Integrated Elastic Intensity
1.0
0.8
0.6
0.4
0.2
50
100
150
200
250
300
Temperature (K)
MBP(H)-PMeEP(H)10 kDa , dry
MBP(H)-PMeEP(H)10 kDa , hydrated

b)

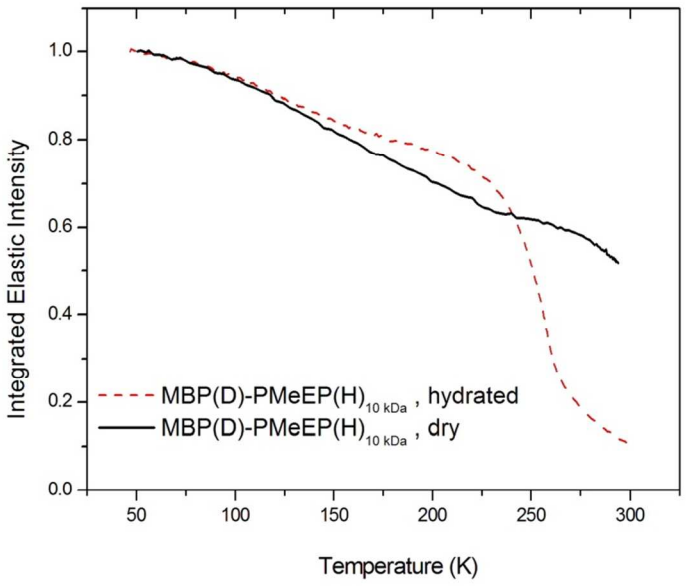
Integrated Elastic Intensity
1.0
0.8
0.6
0.4
0.2
0.0
50
100
150
200
250
300
Temperature (K)
MBP(D)-PMeEP(H)10 kDa , hydrated
MBP(D)-PMeEP(H)10 kDa , dry

c)

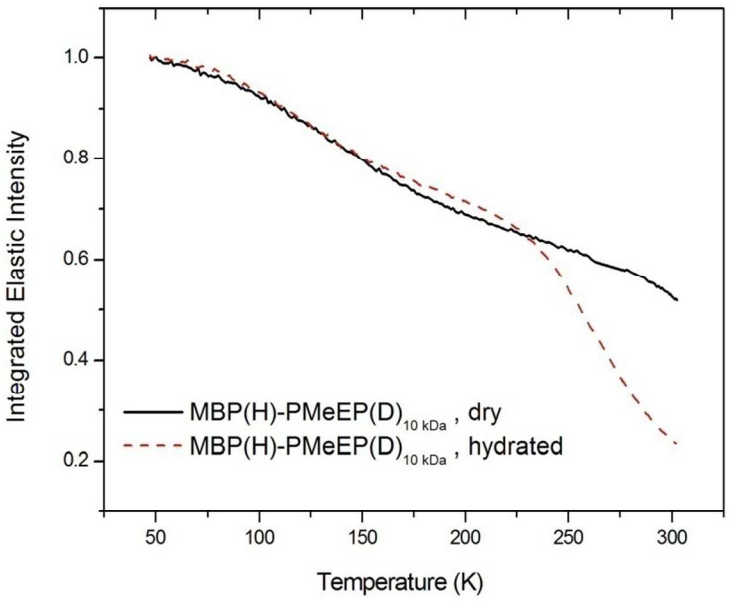
Integrated Elastic Intensity
1.0
0.8
0.6
0.4
0.2
50
100
150
200
250
300
Temperature (K)
MBP(H)-PMeEP(D)10 kDa , dry
MBP(H)-PMeEP(D)10 kDa , hydrated

d)

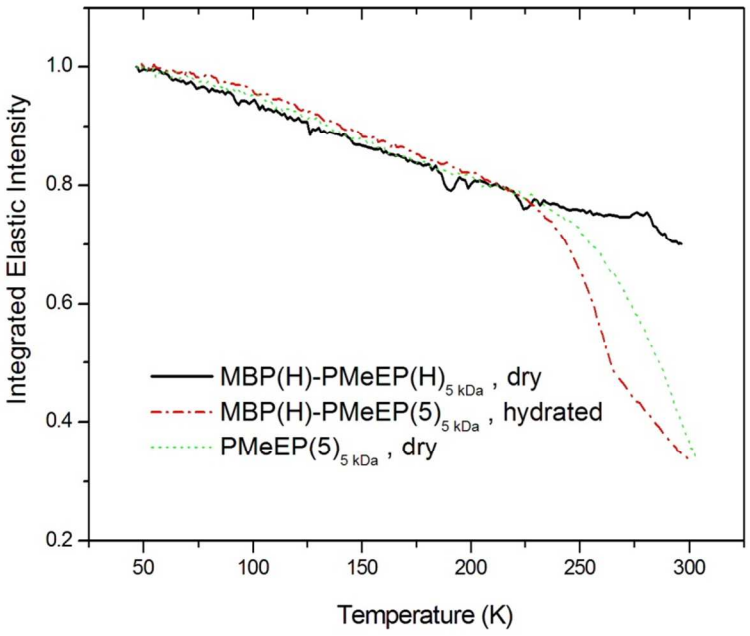

e)

Figure S14:(a-e) *Comparison of the integrated elastic Intensity for all dry and hydrated samples as a function of Temperature. All samples are characteristic of an abrupt drop of Intensity around 225 K.Error bar are reported in panel b) as example for all panels. a) MBP (H); b) MBP(H)-PMeEP(H)$_{10kDa}$; c) MBP(D)-PMeEP(H)$_{10kDa}$; d) MBP(H)-PMeEP(D)$_{10kDa}$; e) MBP(H)-PMeEP(H)$_{5kDa}$ + PMeEP(H)$_{5kDa}$;*

4.5 Quasi-elastic spectra and Relaxation time

Figure S15, shows an example of the collected dynamical incoherent structure factor, S(Q,w), summed over all Q values, for two different samples and the resolution function. The data show a clear quasi-elastic signal and a distinct behavior of the pure native MBP(H) compared to the conjugate MBP(H)-PMeEP(D). The larger is the linewidth the faster is the dynamics.

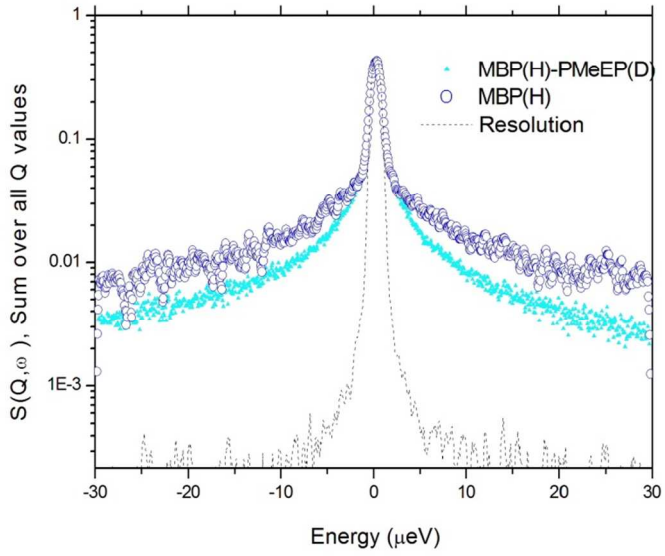

Figure S15*Dynamical incoherent structure factor, S(Q,w), summed over all Q values, for MBP(H) (blue empty circle), MBP(H)-PMeEP(D) (full triangle) and resolution function (dotted line). The spectra are normalized to the maximum of the resolution function*

The relaxation time for the pure dry polymer and the hydrated conjugated at 5kDa are reported in Figure S16. In agreement with the MSD reported in Figure 4 and Figure 5 of the manuscript, the results show that thepolymer molecular weight (between 5 kDa and 10 kDa) does not seem to influence the relaxation time of the hydrated conjugates in theinvestigated timescale (<1.3 ns)

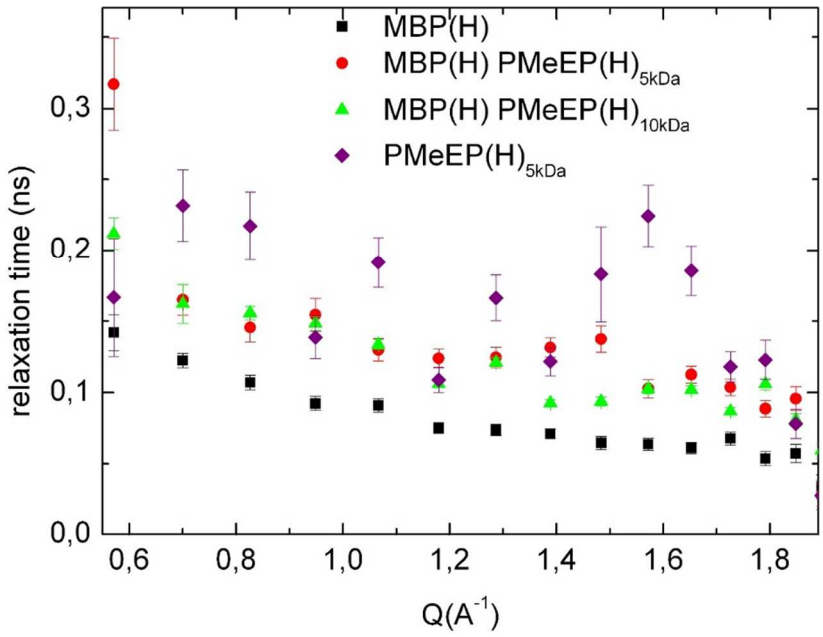

FIGURE S16: *Polymer-protein relaxation time as a function of Q value for hydrated native MBP (full square), completely hydrogenated conjugates at 5 kDa (full circle) and 10 kDa(full triangle) polymer and pure dry polymer at 5 kDa (full diamond)*

5. Calculation of Tg of hydrated polymer.

Many models have been proposed for the prediction of the glass transition temperature of the mixture of amorphous compounds. The most simplistic of these models assume perfect volume additivity at Tg whitout specific interactions. Therefore the glass transition temperature can be written as:

$$T_{g\,mix} = \Phi_1 T_{g1} + \Phi_2 T_{g2}$$

Because of different thermal expansivity $\Delta\alpha$, at Tg, of each component of the mixture, the volume fraction Φ can be written as a function of the weight fraction w: $\Phi = \Delta\alpha . w/\rho$, where ρ is

the density. Then the relation can be expressed as:

$$T_{g\,mix}=[w_1*T_{g1} + K*w_2*T_{g2}]/(w_1+K*w_2) \text{ with } K= \rho_1*\Delta\alpha_2/.\rho_2*\Delta\alpha_1$$

Assuming further that $\Delta\alpha*Tg\sim$constant, then the equation simplifies to give the Gordon-Taylor/Kelley Bueche[13] relation of the same form to the previous one but in which the previous constant K becomes:

$$K=\rho_1*T_{g1} /.\rho_2*T_{g2}$$

If, eventually, the densities are supposed to be equal, then the equation simplifies to lead to the Fox[14] equation

$$1/T_{g\,mix}= w_1/T_{g1}+w_2/T_{g2}$$

References

(1) Spurlino, J.; Lu, G.; Quiocho, F. *J. Biol. Chem.***1991**, *266* (8), 5202.

(2) Sharff, A. J.; Rodseth, L. E.; Spurlino, J. C.; Quiocho, F. A. *Biochemistry***1992**, *31* (44), 10657.

(3) Wood, K.; Frölich, A.; Paciaroni, A.; Moulin, M.; Härtlein, M.; Zaccai, G.; Tobias, D. J.; Weik, M. *J. Am. Chem. Soc.***2008**, *130* (14), 4586.

(4) Artero, J. B.; Härtlein, M.; McSweeney, S.; Timmins, P. *Acta Crystallogr. D. Biol. Crystallogr.***2005**, *61* (Pt 11), 1541.

(5) Steinbach, T.; Ritz, S.; Wurm, F. R. *ACS Macro Lett.***2014**, *3* (3), 244.

(6) Frick, B.; Combet, J.; Van Eijck, L. *Nucl. Instruments Methods Phys. Res. Sect. A Accel. Spectrometers, Detect. Assoc. Equip.***2012**, *669*, 7.

(7) Azuah, R. T.; Kneller, L. R.; Qiu, Y.; Tregenna-Piggott, P. L. W.; Brown, C. M.; Copley, J. R. D.; Dimeo, R. M. *J. Res. Natl. Inst. Stand. Technol.***2009**, *114* (6), 341.

(8) D. Richard, M. F. and G. J. K. *J. Neutron Res.***1996**, *4*, 33.

(9) Bée, M. *Quasielastic Neutron Scattering*; Adam Hilger, 1985.

(10) Paciaroni, A.; Orecchini, A.; Cornicchi, E.; Marconi, M.; Petrillo, C.; Haertlein, M.; Moulin, M.; Sacchetti, F. *Philos. Mag.***2008**, *88* (33-35), 4071.

(11) Orecchini, A; Paciaroni, A. *Phys. B Condens. Matter***2004**, *350* (1-3), E595.

(12) Zanotti, J.-M.; Bellissent-Funel, M.-C.; Chen, S.-H. *EPL (Europhysics Lett.***2005**, *71* (1), 91.

(13). Kelley, F. N.; Bueche, F. *J. Polym. Sci.***1961**, *50*, 549; Gordon, M.; Taylor, J. S. *J. Appl. Chem.***1952**, *2*, 493.

(14). Fox, T. G. *J. Appl. Phys.***1950**, *21*, 581.]: